FT-IR and FT-Raman spectra, *ab initio* and density functional computations of the vibrational spectra, molecular geometry, atomic charges and some molecular properties of the biomolecule 5-iodouracil

V.K. Rastogi [a],*, M. Alcolea Palafox [b], A. Guerrero-Martínez [b], G. Tardajos [b], J.K. Vats [a], I. Kostova [c], S. Schlucker [d], W. Kiefer [d]

[a] Department of Physics, C.C.S. University, Meerut-250 004, India
[b] Departamento de Química-Física I, Facultad de Ciencias Químicas, Universidad Complutense, Madrid-28040, Spain
[c] Department of Chemistry, Faculty of Farmacy, 2 Dunav St., Sofia 1000, Bulgaria
[d] Institut für Physikalische Chemie, Universität Würzburg, D-97074, Würzburg, Germany

ABSTRACT

Density functional calculations (DFT) by various methods were performed to clarify wavenumber assignments of the experimental observed bands. A comparison with the molecule of uracil was made, and specific scale factors were deduced and employed in the predicted wavenumbers of 5-IU. Comparisons were also performed with other halo-uracil derivatives. The scaled wavenumbers were compared with IR and Raman experimental data. Good reproduction of the experimental wavenumbers is obtained and the % error is very small in the majority of cases. The equilibrium geometry of 5-IU was also calculated at several levels, as well as the atomic charges and several thermodynamic parameters. All the tautomer forms of 5-iodouracil were determined and optimized. Several general conclusions were underlined.

© 2009 Published by Elsevier B.V.

1. Introduction

The halogenated pyrimidines have been synthesized in the 1950s as potential antitumor agents after the discovery that certain tumors preferentially incorporated uracil rather than thymine into the DNA [1]. Among these compounds the 5-halogenated uracils have special attention [2]. They have been found to exert profound effects in a variety of microbiological and mammalian systems [3], and they have been used as antitumor [4], antibacterial [5], and antiviral [6] drugs. In this last case, they have been tested against HIV [7] and HSV [8]. Influence of halogenation on the properties of uracil and its noncovalent interactions with alkali metal ions has been also reported [9]. Extensive work, both theoretical and experimental, has been done with the structural analogues of pyrimidine metabolites, i.e. the preparation and properties of oligodeoxynucleotides containing 5-IU [10], the study of alkenyl acyclonucleosides derivatives of 5-halogenouracil as antiviral and antitumoral agents [11] or the photoreactivity of 5-iodouracil (5-IU) containing DNA–Sso7d complex in solution [12]

have been reported. In previous works, we have studied 5-fluorouracil [13], and 5-bromouracil [14] molecules, and other uracil derivatives [15]. Now in order to extend this study further, in the present paper we undertake the study of 5-IU molecule.

5-IU is an important antimetabolite like other halogenated uracils, being in the case of 4-aminobutyrate aminotransferase the most effective inhibitor [4]. For the study of the effects of its incorporation to the RNA [16], and the identification of the binding site of the nucleic acid–protein complexes has been used the photocross-linking technique [17]. Some of 5-IU derivatives have also antitumor activity [18], and have been used in the treatment of hepatitis B infections [19]. Some of 5-IU based nucleoside analogues have been found to be selective inhibitors of herpes simplex viruses [20].

From the spectroscopic point of view, Electronic Absorption [21,22], Thermoluminescence emission [23], Electron Spin Resonance, NMR [24,25], mass electron- and chemical-ionization spectra [26] measurements of 5-IU and other substituted uracils have been reported. The particular interest [27] is due to the biological effects of the radiation on these molecules. The irradiation with ultraviolet light causes changes in the infrared spectrum [28], possibly associated with the formation of loosely associated species.

Thus what is happening is photocleavage of the iodine to make a radical.

It is surprising that the vibrational spectra of 5-IU, taken for low-temperature matrices and for the polycrystalline state, have been looked into relatively little [18,29–32], and that the literature assignments of a number of fundamental vibrations are often in conflict. The assignments of the bands have been mainly based on normal coordinate analysis together with a comparison with the assigned spectrum of uracil. Only Zwierzchowska et al. [30] have reported *ab initio* calculations but of some stretching frequencies, and Dobrowolski et al. [33], the best paper, with calculations at the B3PW91/6-311G** level and Ar matrix spectra of the five 5-halouracil derivatives. However, doubts appear in the assignment of several bands or this assignment is not enough accurate. In the present study we try to clarify the matter with the use of several *ab initio* quantum chemical methods, and accurate scaling procedures. The assignment was performed according to the definition of the normal modes of the uracil molecule [50]. Moreover, we have included a study of its tautomerism for the first time.

2. Experimental

5-Iodouracil (solid state) of spectral grade was purchased from M/s Aldrich Chemical Co (Milwankee, WI, USA) and used as such without any further purification.

The FT-Raman spectrum of 5-iodouracil was recorded at room temperature in the powder form in the region 50–4000 cm^{-1} on a Bruker IFS66 optical bench with an FRA 106 Raman module attachment. The sample was mounted on the sample illuminator using an optical mount and no sample pretreatment was undertaken. The NIR output (1064 nm) of an Nd: YAG laser was used to excite (the probe) the spectrum. The instrument was equipped with a liquid-nitrogen-cooled Ge detector. The laser power was set at 100 mW and the spectrum was recorded over 1000 scans at a fixed temperature. The spectral resolution was 6.0 cm^{-1} after apodisation.

The mid-infrared spectrum of the compound form 400–4000 cm^{-1} was recorded with a Perkin Elmer FT-IR model 1760 X instrument, using the KBr technique with 1 mg sample per 300 mg KBr. For the spectrum acquisition, four scans were collected at 4 cm^{-1} resolution.

3. Computational methods

The calculations were carried out by using semiempirical and *ab initio* quantum chemical methods. As semiempirical methods, AM1 [34] and SAM1 [35] were selected, which are implemented in the AMPAC 5.0 program package [36], being the AM1 also included in the GAUSSIAN 03 package [37]. As *ab initio* methods were utilized the HF and the B3LYP [38], both with the 3-21G** split valence basis set. The use of this small basis set is because for the iodine atom, it is the largest standard gaussian basis set available in the GAUSSIAN. To avoid this limitation, the DGDZVP basis [39], Stevens–Basch–Krauss ECP triple-split basis (CEP-121G) [40], and the Stuttgart–Dresden ECP basis (SDDAll) [41] were also used with the B3LYP method. These basis sets have been previously tested on the uracil molecule.

In all cases, the optimum geometry was determined by minimizing the energy with respect to all geometrical parameters without imposing molecular symmetry constraints. The keywords OPT and FREQ were used for optimization and frequency calculations, respectively with the GAUSSIAN, while the PRECISE and FORCE keywords correspond to the AMPAC 5.0. In the optimization was used the TIGHT criteria of convergence with GAUSSIAN and the GNORM = 0.001 with AMPAC.

4. Results and discussion

4.1. Geometry optimization

The optimized bond lengths and angles in 5-IU using AM1, SAM1, HF and B3LYP methods are given in Table 1, while the label-

Table 1
Optimized and experimental geometrical parameters, bond lengths (in Å) and angles (in degrees) obtained in uracil and 5-iodouracil.

Parameters	5-IU					Uracil[b]		
	AM1	SAM1	HF/3-21G**	B3LYP/DGDZVP	X-ray[a]	B3LYP/DGDZVP	X-ray[c]	Electron diffraction
Bond lengths								
N1–C2	1.4180	1.412	1.3808	1.3939	1.36	1.3955	1.369(2)[d]	1.395(6)[d]
C2–N3	1.3982	1.402	1.3741	1.3865	1.38	1.3857	1.369(2)[d]	1.391(6)[d]
N3–C4	1.4111	1.415	1.3942	1.4109	1.38	1.4140	1.369(2)[d]	1.415(6)[d]
C4–C5	1.4721	1.488	1.4636	1.4722	1.44	1.4614	1.430(3)	1.462(8)
C5=C6	1.3657	1.371	1.3296	1.3557	1.32	1.3532	1.340(2)	1.343(24)
N1–C6	1.3735	1.386	1.3744	1.3778	1.37	1.3786	1.3557[f]	1.396
N1–H	0.9952	0.999	0.9889	1.0131		1.0126	–	1.002[e]
C2=O	1.2477	1.268	1.2093	1.2207	1.20	1.2219	1.230(2)[d]	1.212(3)
C4=O	1.2398	1.255	1.2091	1.2207	1.24	1.2246	1.230(2)[d]	1.211(3)
C–I	2.0076	2.132	2.1044	2.1056	2.11	1.0824		–
Bond angles								
N–C2–N	117.75	116.0	113.17	112.81	114.9	113.12	114.0(1)	114.6(20)
C–N3–C	123.22	125.6	128.36	128.65	126.5	128.04	126.7(2)	126.0(14)
N–C4–C	116.21	114.0	113.38	113.18	113.0	113.62	115.5(1)	115.5(18)
C4–C5=C6	119.67	121.3	119.62	119.68	122.0	119.82	118.9(2)	119.7(21)
C2–N1–H	117.39	117.1	116.04	115.25		115.02	–	115.7[e]
N3–C2=O	122.43	122.6	123.91	124.24	120.2	124.22	122.3[f]	121.6[f]
C4–N3–H	119.43	118.3	115.95	115.78		116.37	–	–
N3–C4=O	117.58	120.2	120.69	120.33	120.1	120.27	119.1[f]	120.2
C4–C5–I	120.47	119.1	117.72	118.43	116.4	118.30	–	118.1[e]
C=C6–H	122.39	123.0	122.36	122.65		122.61	–	122.8[e]

[a] From Ref. [47].
[b] With H11 instead of I11, from Refs. [42,43].
[c] From Ref. [44].
[d] Mean value.
[e] Fixed parameter.
[f] Determined with the data reported in Refs. [42,44].

ling of the atoms is plotted in Fig. 1. For comparison purposes, in the last two columns of Table 1 are collected the values obtained by X-ray and by electron diffraction in the molecule of uracil [42–44]. Although X-ray data of complexes of 5-IU with transition
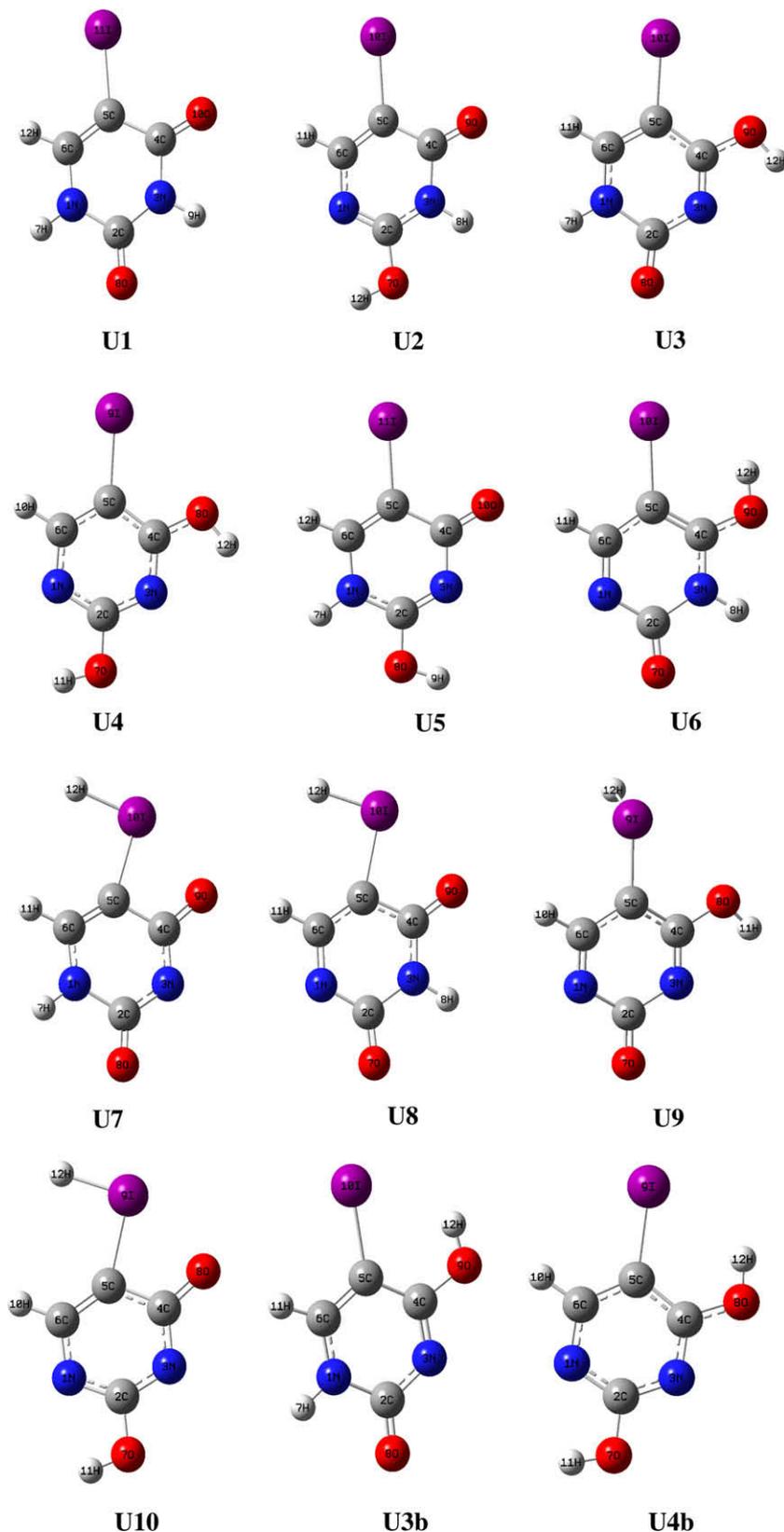
Fig. 1. Structures and labeling of the atoms in the neutral form of 5-iodouracil tautomers. (U1) 2,4-dioxo 5-iodouracil, (U2) 2-hydroxy-4-oxo 5-iodouracil, (U3) 2-oxo-4-hydoxy 5-iodouracil, (U4) 2,4-dihydroxy 5-iodouracil, (U5) 1H-2-hydroxy-4-oxo 5-iodouracil, (U6) 3H-2-oxo-4-hydroxy 5-iodouracil, (U7) 1H-2,4-dioxo 5-iodo(1H)uracil, (U8) 2-oxo-4-hydroxy 5-iodo(1H)uracil, (U9) 3H-2,4-hydroxy 5-iodo(1H)uracil, (U10) 1H-2,4-hydroxy 5-iodo(1H)uracil.

metals [45] and with dihydropyrimidine dehydrogenase [46] have been reported, but only few data appears for 5-IU [47].

The molecule is completely planar, so torsional angles are 0° or 180°, in general accordance to that obtained experimentally, where the 5-IU molecules form planar, H-bonded ribbons stacked. Nevertheless small deviations of the planarity [47] have been reported in the crystal due to the intermolecular H-bonds. The iodine atom also forms a close contact of 3.76 Å with carbon atoms of an adjacent pyrimidine ring, which also deviates this iodine atom from the planarity. The halogen affects the solid state base-stacking patterns, and it has been suggested that stacking interactions involving the halogen may contribute to the unusual physical and biological properties of the molecule.

The iodine atom appears out-of the symmetric axis through the C4–C5 and C5–C6 bonds. The *tilt* angle ε between this axis and the C–I bond, Fig. 2, has the value of 1.7°, very close to that of uracil, 1.8°, calculated at the B3LYP/DGDZVP level as well as the B3LYP/6-311++G(3df,pd). Also the O8 atom appears out-of the symmetric axis through the N1–C2 and C2–N3 angles. The *tilt* angle ε' between this axis and the C2=O8 bond has the small value of 0.6°, also very close to that of uracil, 0.8°. The calculated C–I bond is in accordance with the X-ray value reported in iodobenzene [48], 2.05 ± 0.01 Å.

It is noted that the calculated length of the C–N and C–C single bonds are intermediate between the corresponding aromatic and the saturated bond. Thus some aromatic character is on the ring structure. These values appear overestimated, specially the N1–C2 bond. The values determined by AM1 are in general, ca. 0.005 Å, shorter than those by SAM1, but higher than HF and B3LYP, which are the closest to the electron diffraction results. X-ray data differs remarkably due to the intermolecular bonds.

In the angles, small differences, ca. 2°–4°, are observed with the different methods, being close between HF and B3LYP. The highest differences correspond to the N–C–N and C–N–C bond angles.

4.1.1. Other 5-halouracil derivatives

Several selected calculated geometrical parameters of interest in F-, Cl- and Br-uracils are listed in Table 2. The experimental data
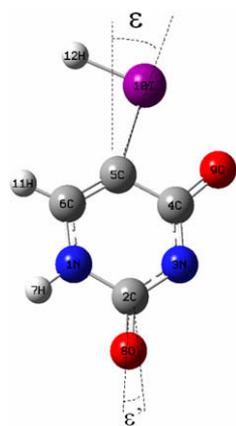
Fig. 2. Definition of the deformation *tilt* angles (ε) in one of the tautomers.

U9
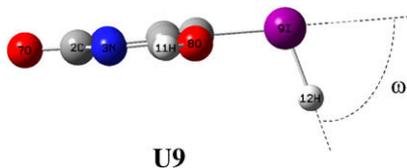
Fig. 3. Other view of the optimized tautomer U10.

Table 2
Optimized geometrical parameters, bond lengths in Å, angles in degrees, calculated at the B3LYP/DGDZVP level in 5-XU derivatives.

X =	F	Cl	Br
C5–X	1.3438	1.7338	1.8950
C4–C5	1.4674	1.4730	1.4719
C5=C6	1.3487	1.3542	1.3541
N3–C4	1.4084	1.4100	1.4110
C2=O	1.2212	1.2208	1.2207
C4=O	1.2202	1.2196	1.2197
C4–C5–X	117.29	118.26	118.36
C4–C5=C6	121.61	120.15	120.20
N3–C4–C5	112.17	112.82	112.79
N1–C2–N3	113.11	112.87	112.87

by X-ray has been reported in 5-FU [49], 5-ClU and 5-BrU [49b] to test these values.

The optimized ring structure of these molecules is planar, in agreement with their experimental data available on uracil and 5-fluorouracil (5-FU). With the 5-substitution on the uracil ring, several key effects and certainly inter-related, can be underlined that produces the marked differences in the biological and pharmacological activities of these nucleobases:

(i) The first effect, and the most important, is the drastic change of their functional ones expressed in terms of intermolecular interactions. With the increase of the electronegativity of the halogen atom is produced an increment in the perturbation in the electronic environment of the heterocyclic ring, and the new possibility of intermolecular H-bonds through this halogen atom. It also increases the polarizability of the nucleobases. The calculated natural atomic charge on the fluorine atom was −0.36, while on the chlorine and bromine atoms was 0.006 and 0.09, respectively, and on the iodine atom 0.22.

It is noted that in 5-FU the fluorine atom withdraws electrons from C5 atom, and it changes from a negative charge, −0.37 in uracil, to a positive charge of 0.31 in 5-FU. Consequently, the positive charge on the C4 and C6 atoms is reduced in 5-FU by 0.05 and 0.09, respectively.

In 5-chlorouracil (5-ClU) and 5-bromouracil (5-BrU), with a small positive charge of the halogen atom, the reduction of the negative charge on C5 atom is much lower than in 5-FU. The charge on C5 atom is −0.16 in 5-ClU and −0.25 in 5-BrU. This fact leads to more close geometric parameters with uracil than with 5-FU.

In 5-IU the charge on the iodine atom (0.22) is very close to the related hydrogen atom of the uracil molecule, 0.24. This fact leads to similar atomic charges on C5, −0.39 vs. −0.37 of uracil, and on C4, 0.71 vs. 0.72 of uracil, and C6, 0.08 vs. 0.09 of uracil; and consequently the *ipso* angle C4–C5=C6 is similar, 119.7° vs. 119.8° in uracil, while in 5-ClU and 5-BrU are 120.15° and 120.2°, respectively.

(ii) From 5-FU to 5-IU, the C4–C5–X and C6–C5–X angles are in general opened which produce a reduction of the *tilt* ε angle, from 1.9° in 5-FU to 1.7° in 5-ClU and 1.5° in 5-BrU. 5-IU is an exception, and the ε angle increases to 1.7°. The C4–C5–X angle is always lower (from 3.1° to 3.8°) than the C6–C5–X angle.

The N1–C2–O8 angle is always higher than the N3–C2–O8 angle, from 0.6° to 1.6°. The *tilt* ε angle is very low in 5-FU, 0.3°, while in 5-ClU, 5-BrU and 5-IU has the same value, 0.6°.

(iii) Other small effects appear with the substitution, in special from 5-FU to 5-ClU, such as, a small increase of the C4–C5 and N3–C4 bonds and a shortening of the C4=O bond, while the C2=O, N1–C2 and C2–N3 bonds remain almost unchanged. This fact produces a slightly closening of the *ipso* angle C4–C5=C6, ∼1.5°, and opening of the N3–C4–C5 angle, ∼0.6°, while the N1–C2–N3 angle is little affected, 0.2°.

4.2. Vibrational wavenumbers

The scaled IR and Raman spectra of 5-IU are reproduced in Figs. 4–7. The study is divided in the 3550–3350 cm^{-1} range, Figs. 4 and 5 corresponding to the IR and Raman spectra, respectively, and in the 2000–50 cm^{-1} range, Figs. 6 and 7 corresponding to IR and Raman, respectively. For comparison purposes, in the bottom of Figs. 6 and 7 are shown experimental spectra. The molecule under study belongs to the C_s point group with the normal mode distribution 21a′ + 9a″. According to the selection rules, both a′ and a″ vibrations are allowed in Raman and IR spectra. a′ vibrations are totally symmetric and gives rise to depolarized Raman lines.

The harmonic vibrational bands computed with the quantum chemical methods used are shown in Table 3. The first column lists the calculated wavenumbers (in cm^{-1}) with AM1, while the second column collects their relative infrared intensities (A) in %. They were obtained by normalizing the computed value to the intensity of the strongest band, the ν(C2=O) mode in 5-IU. Similar results were determined using the SAM1 method, columns 3–4th. With HF calculations were obtained the relative Raman intensities (S), 7th column. With the B3LYP method and different basis set were obtained the values of columns 8–17th. The Raman depolarization ratios for plane polarized (P) and unpolarized (U) incident light, and the force constant (f) in mDyne/Å, are shown in the 15–17th

columns, respectively. The values reported [33] at the B3PW91/6-31G** level is shown in the 18th column. In the last two columns appear the characterization of the local modes of 5-IU using the definition of the ring normal modes of uracil [50]. The calculated % Potential Energy Distribution (PED) of the different modes for each vibration corresponds to B3LYP/DGDZVP. Similar results were determined with the other methods. Contributions lower than 10% were not considered.

An improvement can be carried out on the computed wavenumbers by the use of scaling procedures. To scale the wavenumbers, the simplest procedure is using an overall scale factor [51], which is the procedure generally used in the literature [52], but it leads to a high error in the scaled values and impede a clear and accurate assignment.

Thus to reduce this error and get a trustworthy assignment two accurate scaling procedures were employed [51], Table 4, the scaling equation and the specific scale factors for each mode. Both procedures require the previous calculated wavenumbers of the uracil molecule [50] determined at the same computational level. For convenience, the 2nd–5th columns of this Table collect the specific scale factors obtained for uracil molecule. With them and using the scaling equations were determined the scaled wavenumbers shown in the 6–14th columns. These values in 5-IU can be directly compared with the experimental infrared and Raman data reported
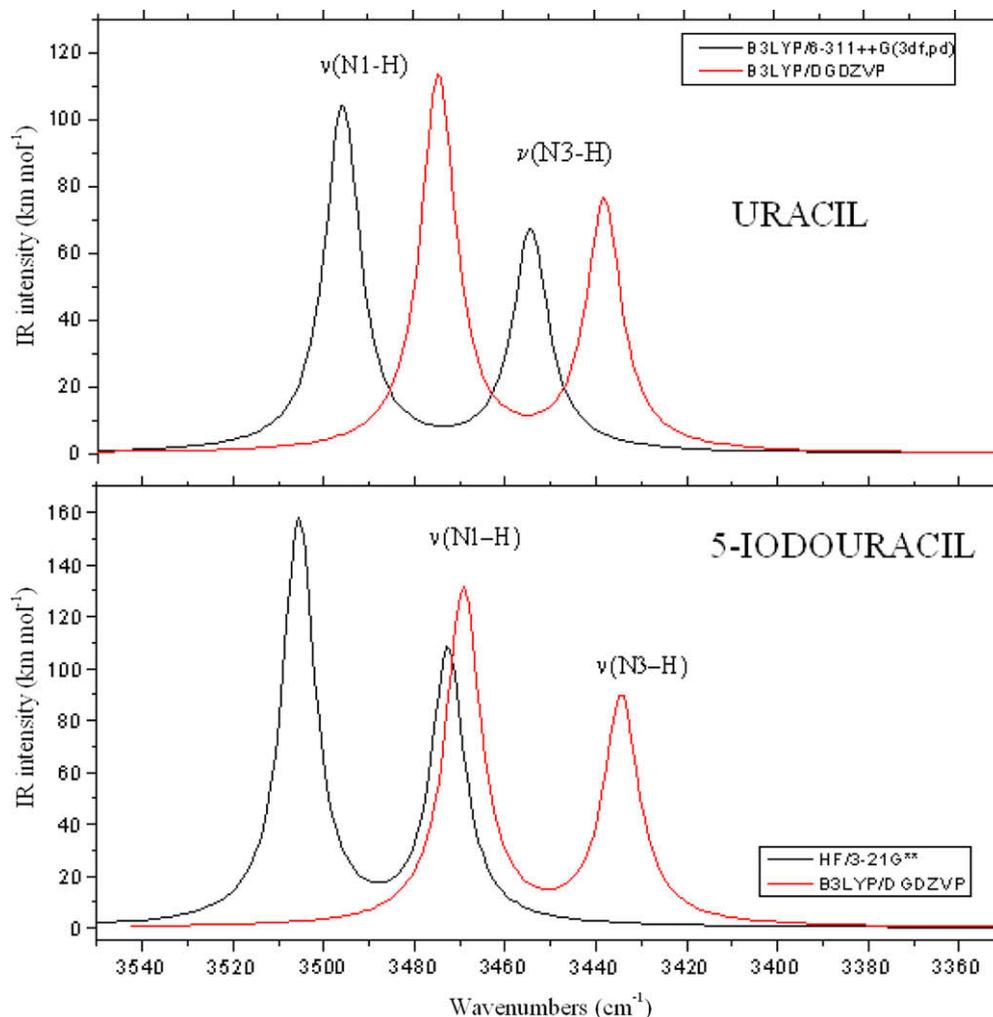
Fig. 4. Theoretical scaled IR spectrum in the 3550–3350 cm^{-1} range using the scale equation procedure with uracil molecule at B3LYP/6-311++G(3df,pd) and B3LYP/DGDZVP levels, and with 5-iodouracil molecule at B3LYP/DGDZVP and HF/3-21G* levels. The scale equations used were $\nu_{\text{scaled}} = 31.9 + 0.9512 \cdot \nu_{\text{calculated}}$ for B3LYP/6-311++G(3df,pd) level, $\nu_{\text{scaled}} = 39.2 + 0.9472 \cdot \nu_{\text{calculated}}$ for B3LYP/DGDZVP level, and $\nu_{\text{scaled}} = 7.7 + 0.8795 \cdot \nu_{\text{calculated}}$ for HF/3-21G** level.
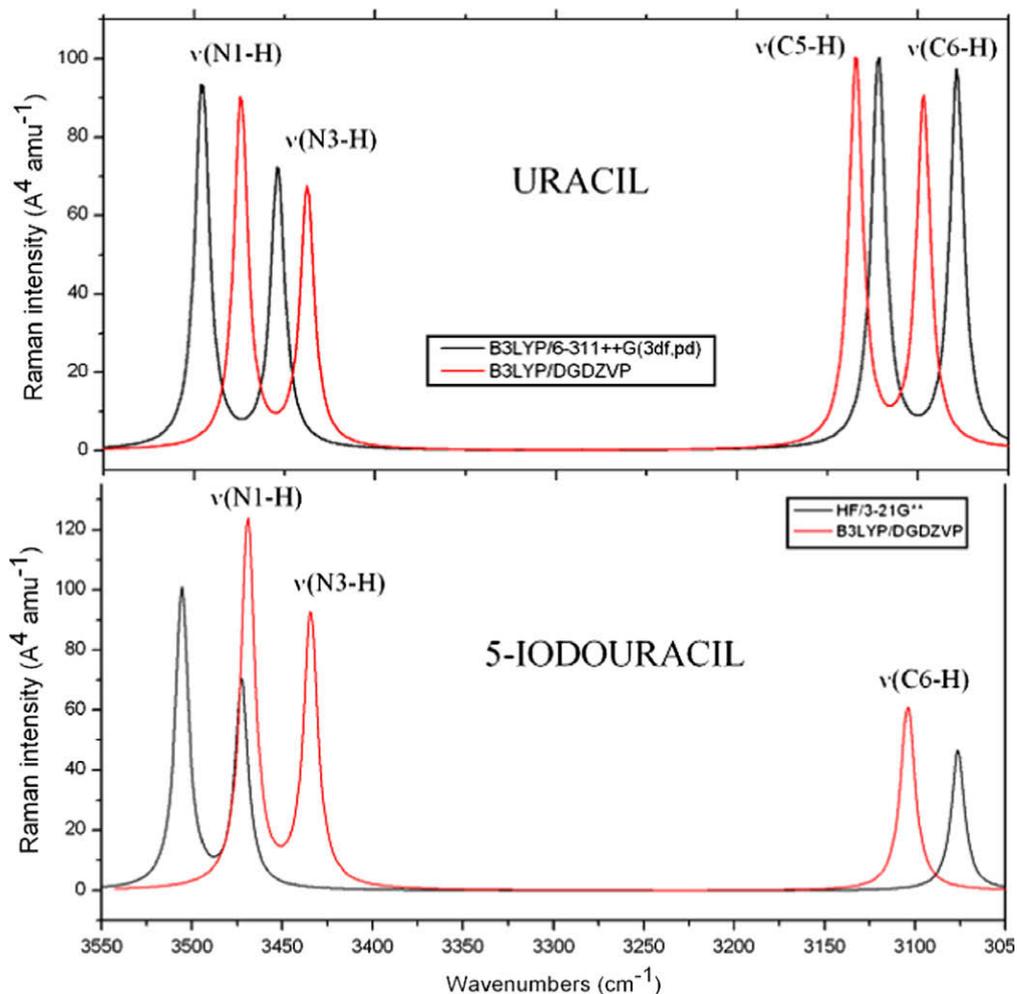
Fig. 5. Theoretical scaled Raman spectrum in the 3550–3350 cm^{-1} range using the scale equation procedure with uracil molecule at B3LYP/6-311++G(3df,pd) and B3LYP/DGDZVP levels, and with 5-iodouracil molecule at B3LYP/DGDZVP and HF/3-21G* levels.

in literature by Kumar et al. [29], Zwierzchowska et al. [30] and Dobrowolski et al. [33], listed in the columns 16–18th and 20th. The specific scale factors for each mode procedure leads to the lowest errors, although it requires more effort and with high basis set the difference is insignificant. Thus for simplicity with the DGDZVP, CEP and SDAll basis was only used the scaling equation procedure.

In uracil molecule the linear regression between the calculated and experimental wavenumbers with the DGDZVP basis set gives a correlation coefficient of 0.9998 more close to 1 than that obtained with the CEP and SDAll basis set, 0.9992 and 0.9990, respectively. Also the standard deviation is lower, 16.2 with DGDZVP, while it is 36.7 with CEP and 40.6 with SDAll. With the larger 6-311++G(3df,pd) gaussian basis set was obtained a correlation coefficient of 0.9998, and a standard deviations of 15.8, very close to the results with the DGDZVP basis, 16.2. For this reason, the results with this basis set was selected for the discussion in the present study.

An analysis of the different vibrations is as follows.

4.2.1. C=O modes
4.2.1.1. Stretching modes. The carbonyl stretching region is somewhat peculiar and C=O modes are the most important modes of nucleic acid base derivatives, because they take part in hydrogen bonding. Therefore, comparison of C=O stretching wavenumbers in different nucleic acid base derivatives has been reported [53].

The pattern of the C=O bands in uracil and its derivatives is always very complex. Usually the two C=O modes split into several peaks. It is believed that the Fermi resonance of fundamentals with combination bands is responsible for this splitting. In the present study with 5-IU molecule, the two strong IR bands at 1783 and 1747 cm^{-1} have been identified as ν(C2=O) mode (ring normal mode no. 26 in uracil [50]) and that at 1700 cm^{-1} as ν(C4=O) mode (ring normal mode no. 25), in accordance with those reported [33] in Ar matrix at 1765.5 and 1761.5 cm^{-1} for ν(C2=O) and at 1722.5, 1706.5 cm^{-1} for ν(C4=O). The corresponding bands in the Raman spectrum appeared at 1765 and 1715 cm^{-1}. These modes appear coupled with δ(N–H) modes, although the calculated degree of coupling change slightly among the different DFT methods used. Thus the scaled band by B3LYP/DGDZVP at 1756.4 cm^{-1} has been assigned to ν(C2=O) and coupled ca. 12% with δ(N3–H) and 11% with δ(N1–H), while the scaled band at 1716.6 cm^{-1} has been assigned to ν(C4=O) and coupled ca. 20% with δ(N3–H). The coupling between the C=O groups is less than 5%. The semiempirical methods fail in this sense with this group, as well as in calculating at higher wavenumber the ν(C4=O) than the ν(C2=O).

The absence of a ν(OH) band in the 3500–3700 cm^{-1} range and the appearance of ν(C=O) modes as strong bands in the 1600–1750 cm^{-1} range, indicate that in the solid state the molecule exists in the keto form.

Regardless of the C5 substitution, the ν(C2=O) band's position is predicted to remain almost unaffected by changes in the molec-

ular structure of the uracil ring. This is caused by the fact that the C2=O group is quite distant from the C5–I group and, moreover, it is surrounded by the two N–H groups, which buffer it from influences of the remaining molecular moieties. On the other hand, the C4=O moiety neighbors the C5–I group, and as the halogen mass is increased, the corresponding v(C4=O) harmonic mode drifts slightly towards lower wavenumbers, from 1786 cm^{-1} for 5-FU to 1781 cm^{-1} for 5-ClU, 1778 cm^{-1} for 5-BrU, and 1771 cm^{-1} for 5-IU.

The two band intensities are practically equal for uracil and 5-FU. For heavier halogens, the v(C2=O) IR band intensity increases, whereas the v(C4=O) band intensity decreases proportionally so that, for the 5-IU molecule, the former is twice as intense as the latter, as can be seen in Table 3 with all the theoretical methods used, although by AM1 is ca. five times higher. This C2=O IR band intensity is the highest in the spectrum in accordance with that observed experimentally.

However, the C2=O Raman intensity calculated by DFT methods is ca. three times lower than v(C4=O) in U and 5-FU, in contradiction with the experimental Raman spectrum [13] of 5-FU where the intensity of the v(C2=O) mode is higher than v(C4=O). By contrast HF reproduces well the Raman intensity pattern in this case. For this reason the simulation of the Raman spectra by HF was included in Figs. 5 and 6. In 5-IU the Raman intensity by DFT methods of the v(C2=O) mode is calculated slightly lower than of the

Fig. 7. Theoretical scaled Raman spectrum in the 2000–50 cm^{-1} range using the scale equation procedure with uracil molecule at B3LYP/6-311++G(3df,pd) and B3LYP/DGDZVP levels, and with 5-iodouracil molecule at B3LYP/DGDZVP and HF/3-21G* levels. In the bottom is experimental Raman spectrum of 5-iodouracil in the range 50-2000 cm^{-1}.

v(C4=O), while by HF the intensity of the v(C2=O) mode is ca. two times lower than that of the v(C4=O).

4.2.1.2. In-plane bending modes. The δ(C=O) local mode, ring mode no. 6, appears characterized by its strong coupling with the δ_{as}(ring) mode, and it was calculated at 625.7, 601.3, 592.7 and 586.8 cm^{-1} for the 5-FU, 5-ClU, 5-BrU and 5-IU molecules, respectively, in accordance with the reported [33] values by B3PW91/6-311G** level at 630, 605, 600 and 590 cm^{-1}. The analogous mode in U is predicted to absorb at 539.1 cm^{-1}. The theoretical IR intensity of the mode is weak in all the spectra studied, and for 5-ClU it is practically inactive. The theoretical Raman activity of the mode is weak. The low experimental intensity of this mode is the reason why the investigators have had difficulties in assigning the band in halouracil spectra.

The another δ(C=O) mode, ring mode no. 3, appears also characterized by its strong coupling with a δ(ring) mode. Analogously, it is also calculated with weak IR and Raman intensity. Its wavenumber at 392.6 cm^{-1} in 5-IU is analogous to that calculated in 5-BrU at 393.2 cm^{-1}. However, this mode appears coupled with the v(C–X) mode in 5-FU and 5-ClU, shifting to 386.5 and 402.2 cm^{-1}, respectively. In uracil it was calculated at 384.2 cm^{-1}.

4.2.1.3. Out-of-plane bending modes. The two γ(C=O) out-of-plane bending vibrations are also coupled strongly with ring modes, in contradiction to the coupling reported by Dobrowolski et al. [33]

Fig. 6. Theoretical scaled IR spectrum in the 2000–50 cm^{-1} range using the scale equation procedure with uracil molecule at B3LYP/6-311++G(3df,pd) and B3LYP/DGDZVP levels, and with 5-iodouracil molecule at B3LYP/DGDZVP and HF/3-21G* levels. In the bottom is experimental IR spectrum of 5-iodouracil in the range 400–2000 cm^{-1}.

Table 3

Comparison of the calculated harmonic wavenumbers (ω, cm^{-1}), relative infrared intensities (A, %), relative Raman scattering activities (S, %), Raman depolarization ratios for plane (P) and unpolarized (U) incident light and force constants (f, mDyne/Å) obtained in 5-iodouracil with different quantum chemical methods.

AM1		SAM1		HF/3-21G**			B3LYP/ 3-21G**		CEP-121G	SDDAll	DGDZVP						B3PW91[a]	Ring no.	Characterization
ω	A	ω	A	ω	A	S	ω	A	ω	ω	ω	A	S	P	U	f	ω		
3458	29	3464	0	3977	20	100	3707	21	3614	3634	3621.2	15	100	0.22	0.37	8.34	3486.5	30	99%, ν(N1–H)
3438	23	3436	0	3940	14	69	3668	12	3576	3599	3584.5	10	74	0.28	0.43	8.16	3441.4	29	99%, ν(N3–H)
3113	7	2890	1	3489	0	47	3311	0	3207	3266	3235.6	0	50	0.34	0.51	6.75	3080.9	27	99%, ν(C6–H)
1997	100	1906	100	1954	100	9	1794	100	1698	1713	1812.9	100	21	0.20	0.33	15.67	1814.1	26	70%, ν(C2=O) + 12%, δ(N3–H) + 11%, δ(N1–H)
2039	23	1970	38	1926	61	22	1742	45	1659	1681	1770.9	54	25	0.37	0.54	18.04	1765.0	25	80%, ν(C4=O) + 15%, δ(N3–H)
1788	42	1824	36	1808	19	33	1653	11	1620	1649	1658.5	10	51	0.19	0.32	9.23	1636.0	24	67%, ν(C5=C6) + 16%, ν(C2–N3) + 14%, ν(C–N1–C)
1621	26	1621	21	1615	7	10	1476	6	1463	1491	1487.4	9	11	0.58	0.73	3.51	1458.0	23	79%, δ(N1–H) + 14%, ν(C–C6–N)
1526	18	1542	11	1500	31	4	1343	22	1406	1430	1408.7	10	3	0.57	0.73	3.07	1374.7	21	40%, ν(CN3C) + 35%, δ(N3H) + 13%, ν(C=C6H) + 11%, δ(N1–H)
1496	1	1453	7	1566	0	3	1420	0	1380	1407	1397.5	6	0	0.74	0.85	2.29	1373.4	20	34%, δ(N3–H) + 31%, ν(C–N) + 23%, δ(N1–H)
1436	1	1379	1	1479	10	24	1373	15	1344	1370	1350.2	2	22	0.31	0.47	1.95	1316.5	22	40%, δ(C6–H) + 24%, δ(C=C6) + 15% δ(C–N) + 11%, δ(N1–H)
1359	0	1265	0	1306	12	3	1180	18	1198	1215	1201.7	9	2	0.68	0.81	1.75	1173.4	18	28%, ν(C–N) + 28%, δ(C6–H) + 24%, δ(N1–H) + 19%, δ(N3–H)
1297	4	1218	3	1230	9	1	1129	0	1148	1163	1161.6	3	2	0.74	0.85	2.50	1140.9	17	58%, ν(ring) + 23%, δ(N1–H)
1150	1	1118	14	1140	4	7	1047	5	1017	1041	1033.8	5	2	0.36	0.53	4.33	1020.3	16	100%, δ(ring) mainly on C5
1087	0	1080	3	1038	2	2	949	3	956	978	974.3	2	2	0.73	0.84	1.68	962.9	14	35%, ν(NCN) + 21%, δ(N3–H) + 16%, δ(C6–H) + 10%, δ(N1–H)
944	0	893	0	1132	0	5	975	1	931	955	917.9	2	1	0.75	0.86	0.68	901.1	15	95%, γ(C6–H)
890	0	887	2	828	0	13	765	0	752	774	770.9	0	24	0.11	0.20	3.13	771.5	12	100%, ν(ring)
777	11	636	0	991	43	1	865	28	783	845	760.8	2	0	0.75	0.86	3.53	758.7	10	46%, γ(C4=O) + 44%, γ(CCN3) + 10%, γ(ring)
718	5	690	0	892	2	4	797	5	733	765	747.7	5	0	0.75	0.86	3.68	755.7	11	80%, γ(C2=O) + 20%, γ(ring)
603	22	664	2	811	1	6	737	3	699	732	663.9	11	2	0.75	0.86	0.29	657.8	9	75%, γ(N3–H) + 16%, γ(N1–H)
654	1	648	5	670	4	1	613	5	595	612	609.5	4	1	0.73	0.84	1.60	606.3	7	100%, δ_{as}(ring)
606	0	588	0	645	1	7	593	0	570	587	586.8	1	5	0.24	0.39	1.40	587.4	6	57%, δ(ring) + 43%, δ(C=O)
496	10	512	1	709	15	2	646	16	629	659	547.3	6	0	0.75	0.86	0.20	563.4	8	75%, γ(N1–H) + 16%, γ(N3–H)
544	1	572	1	585	2	4	530	2	523	540	534.0	1	3	0.24	0.39	1.38	530.4	5	100%, δ(ring)
394	3	415	0	432	4	2	391	3	375	386	392.6	2	2	0.60	0.75	1.12	393.1	3	74%, δ(C=O) + 26%, δ(ring)
401	7	342	1	478	2	2	431	3	400	422	382.9	3	2	0.75	0.86	0.26	385.0	4	100%, γ(ring)
256	0	238	0	308	0	0	276	0	265	281	249.2	0	0	0.75	0.86	0.41	252.9	2	100% puckering N1
263	0	252	0	260	0	7	243	0	231	235	238.5	0	4	0.31	0.47	0.53	239.9		70%, ν(C–I) + 30%, δ(ring)
168	0	130	0	172	0	1	158	0	156	159	156.8	0	1	0.75	0.86	0.17	158.0		80%, δ(C–I) + 20%, δ(ring)
141	0	145	0	200	0	0	176	0	162	170	141.6	0	0	0.75	0.86	0.11	150.0	1	100% puckering N3
68	0	69	0	96	0	0	89	0	83	85	80.5	0	0	0.75	0.86	0.04	81.3		59%, γ(C=O) + 29%, γ(C–I) + 12%, γ(ring)

[a] Ref. [33].

Table 4
Scaled and experimental wavenumbers (v, cm^{-1}) obtained in 5-IU with different procedures.

Ring no.	Scale factors				Scaled frequencies										Experimental				Raman[f]
					Semiempirical		HF		B3LYP					B3PW91[n]	IR				
	AM1	SAM1	HF	B3LYP	AM1	SAM1	3-21G**[a]	3-21G**[b]	3-21G**[c]	3-21G**[d]	CEP[d1]	SDAll[d2]	DGDZ[d3]	6-311G**	Matrix[e]	Matrix[n]	Solid[f]	Solid	Solid
30	1.0043	1.0055	0.8743	0.9383	3473	3483	3505	3477	3506	3478	3499	3481	3469.2	3514.0	3469.9	3470.0			
29	0.9965	0.9985	0.8708	0.9360	3426	3431	3473	3431	3470	3433	3462	3448	3434.4	3476.4	3426.0	3426.0			
27	0.9809	1.0707	0.8842	0.9321	3054	3094	3076	3085	3135	3086	3108	3130	3104.0	3102.0			3086[i]	3106 m, 3086 m	3087[j]
26	0.8851	0.9274	0.9005	0.9799	1768	1768	1726	1760	1714	1758	1661	1651	1756.4	1792.4	1765.4[h]	1765.5, 1761.5	1760[g]	1747, 1783 s	1765[g]
25	0.8538	0.8865	0.8997	0.9915	1741	1746	1702	1733	1665	1727	1624	1619	1716.6	1749.6	1723.1	1722.5, 1706.5	1720[g]	1700	1715[g]
24	0.9082	0.9037	0.9002	0.9815	1624	1648	1598	1627	1581	1622	1587	1589	1610.1	1619.7			1630[k]	1606 vs, 1652 vs, br	1640[l]
23	0.9053	0.9047	0.9024	0.9825	1467	1467	1428	1457	1416	1450	1436	1438	1448.1	1458.0		1453.0	1455	1465 s, 1508 sh	1472
21	0.9254	0.9443	0.9259	1.0221	1412	1456	1385	1389	1363	1373	1381	1380	1373.5	1378.1		1392.5	1420	1431 s	1410
20	0.9418	0.9834	0.8681	0.9617	1409	1429	1327	1359	1291	1366	1356	1358	1362.9	1368.5		1384.0		1400 m?	
22	0.8806	0.9545	0.9120	0.9804	1265	1316	1308	1349	1319	1346	1322	1323	1318.1	1314.7		1328.0	1338	1323 s	1340
18			0.9008	1.0034			1156	1177	1138	1184	1182	1175	1177.4	1174.6		1189.5, 1186.0	1228	1215 vs, 1225 sh	1215
17	0.9228	0.9729	0.9274	0.9991	1197	1185	1089	1141	1090	1128	1134	1125	1139.5	1145.6		1149.0		1137 vs	
16	0.9101	0.9363	0.9124	0.9920	1047	1047	1010	1040	1014	1039	1008	1009	1018.4	1019.6		1029.5		1022 sh, 1046 s	
14	0.8937	0.9038	0.9297	1.0117	971	976	921	965	922	960	950	949	962.1	961.7		964.5		996 m	
15	1.0094	1.0513	0.8265	0.9419	953	939	1003	936	946	918	926	927	908.6	907.9		904.0	910	939 s	
12	0.8547	0.8518	0.9290	0.9961	761	756	736	769	749	762	784	822	769.4	775.7		756.5	760	756 vs, 776 s	750
10			0.8546	0.9422			879	847	843	815	754	754	759.8	769.6			810?	849 m, 884 m	
11	1.1198	1.1635	0.7985	0.9023	804	803	792	712	779	719	736	746	747.4	761.0		752.5	740	732 vs	732
9	1.0997	0.9750	0.8209	0.8943	663	647	721	666	723	659	703	714	668.0	678.1		657.5	670	669, 636 vs	668
7	0.9270	0.9286	0.9179	1.0072	606	602	597	615	607	617	604	600	616.5	614.0		607.5	615		620, 640
6	0.9693	0.9537	0.9147	1.0075	587	561	575	590	588	597	580	576	595.0	595.1			–	598 m	
8	1.1849	1.0436	0.7709	0.8463	588	534	631	547	638	547	636	645	557.6	577.6				551 vs	
5			0.9030	0.9865			522	528	529	523	535	531	545.0	540.0		551.0	540	543 vs	550
3			0.9332	1.0317			388	403	399	403	393	384	411.1	407.8					
4			0.8212	0.8937			428	393	436	385	417	419	401.9	399.6			430	428 vs	422
2			0.8894	1.0000			279	274	291	276	287	284	275.2	269.8			420		
	–	–			–	–	236		260		255	240	265.1	258.1					245[m]
	–	–			–	–	159		181		183	168	187.7	178.3			235		
1							184		198		188	178	173.3	171.0					140
	–	–			–	–	92		116		113	97	115.4	105.9					75

[a] With the scaling equation $v_{scaled} = 7.7 + 0.8795 \cdot v_{calculated}$.
[b] With the specific scale factors of the column 4th.
[c] With the scaling equation $v_{scaled} = 32.6 + 0.9370 \cdot v_{calculated}$.
[d] With the specific scale factors of the column 5th.
[d1] With the scaling equation $v_{scaled} = 33.1 + 0.9589 \cdot v_{calculated}$.
[d2] With the scaling equation $v_{scaled} = 16.3 + 0.9535 \cdot v_{calculated}$.
[d3] With the scaling equation $v_{scaled} = 39.2 + 0.9472 \cdot v_{calculated}$.
[e] In Ar Matrix, Ref. [30].
[f] In the solid state, Ref. [29].
[g] Determined in the present work.
[h] And at 1761.3 cm^{-1}.
[i] And at 3048, 3056 cm^{-1}, Ref. [31].
[j] And at 3060 cm^{-1}, Ref. [31].
[k] And at 1606 cm^{-1}, Ref. [31].
[l] And at 1608 cm^{-1}, Ref. [31].
[m] From Ref. [31].
[n] In Ar Matrix, Ref. [33].

with the another $\gamma(C=O)$ mode. The $\gamma(C4=O)$ mode (no. 10) is predicted to occur at ca. 760.8 cm^{-1}, while the analogous wavenumber in U is predicted to occur at ca. 720 cm^{-1} and has a significant contribution (PED ca 20%) in $\gamma(C5-H)$ mode. The calculated IR intensity of this mode is weak and exhibits a tendency to increase as the halogen mass increased. The Raman activity is predicted to be very weak or null. The band does not appear to be affected by halogen substituents.

The $\gamma(C2=O)$ mode (no. 11) is predicted to occur at ca. 747.7 cm^{-1}. The theoretical IR intensity tends to decrease from U to 5-IU and is predicted to be ca. two to three times higher than that of the $\gamma(C4=O)$ mode. Raman activity is predicted to be almost zero.

4.2.2. Overtones and combination bands

The experimental wavenumbers detected in the IR of 5-IU at 1871 (m), 1919 (vw), 1949 (w), 1986 (w), 2053 (vw), 2091 (w,br), 2134 (sh), 2209 (sh), 2275 (sh), 2315 (vw), 2366 (w), 2422 (w), 2467 (w), 2537 (sh), 2603 (sh,br), 2676 (sh,br), 2750 (w), 2824 (s) and 2880 cm^{-1} (sh) were not assigned, as they correspond to overtones and combination bands.

Out of four of the publications on IR spectra of halouracils in cryogenic matrices [33,54–56] only Nowak [54] and Dobrowolski et al. [33] explained the knotty pattern of the $\nu(C=O)$ region in terms of a Fermi Resonance; the origin of the resonance remained unresolved, however. The most reasonable is the one that assigns the $\delta(N3-H) + \delta_{as}(C=O)$ combination tone as resonating with a $\nu(C=O)$ mode.

4.2.3. C=C modes

The stretching $\nu(C5=C6)$, ring mode no. 24, was calculated at 1720.4 cm^{-1} in 5-FU. Its wavenumber shift toward lower values with an increase in the halogen mass from 1676.0 cm^{-1} for 5-ClU, 1669.0 cm^{-1} for 5-BrU, to 1658.5 cm^{-1} for 5-IU. For unsubstituted uracil, the band is calculated to occur at 1678.7 cm^{-1}, a position that agrees very well with the literature value [57] of 1643 cm^{-1}. The PED analysis suggests that the $\nu(C5=C6)$ mode is ca. 70% pure. This means that the $\nu(C5=C6)$ vibration is coupled to the $\nu(C-N)$ mode for a value of, at most, 30%.

The position of the C=C stretching vibrations bands in the experimental spectra is in agreement with those in the theoretical prediction. In the case of unsubstituted uracil, the band (at 1643 cm^{-1} in Ref. [57]) appeared too weak to be detected in the measured spectra.

Unlike the band frequency, the IR intensity is predicted to increase with the halogen mass from ca. 42 km/mode for 5-FU to ca. 90 km/mol for 5-IU.

4.2.4. Ring modes
4.2.4.1. Stretching modes.
The C–N and C–C stretchings correspond to 21, 18, 17, 14 and 12 ring modes. The description of mode 21 is complex. Mainly it is characterized as $\nu(C-N3-C)$ strongly coupled with $\delta(N3-H)$ and with some contribution of the $\nu(C=C-H)$ and $\delta(N1-H)$ modes.

The C–N mode no. 18 is predicted to occur in the 1180–1150 Cm^{-1} range. Its wavenumber increases with the halogen mass, 1192.0 cm^{-1} (5-FU), 1199.8 cm^{-1} (5-BrU), 1200 cm^{-1} (5-ClU). In 5-IU it was calculated at 1201.7 cm^{-1} (scaled at 1177.4 cm^{-1}) in accordance to the IR bands in Ar matrix at 1189.5 and 1186.0 cm^{-1}, and in the solid state at 1215 cm^{-1}. In uracil molecule the mode is calculated at 1201.7 cm^{-1}. The IR intensity of the band is medium and is little affected by substitution at the C5 atom.

Mode no. 17 appears coupled with the $\delta(N1-H)$ vibration. Its wavenumber decreases with the halogen mass. Thus it was computed at 1173.4 cm^{-1} in 5-ClU, at 1165.9 cm^{-1} in 5-BrU, and at

1161.6 cm^{-1} (scaled at 1139.5 cm^{-1}) in 5-IU. This value is in accordance to the strong IR band observed in the solid state at 1137 cm^{-1}.

Mode 14 is defined as antisymmetric stretching of the opposite C4–C5 and N1–C2 bonds, and it is predicted to occur near 960 cm^{-1}. Its wavenumber is practically not affected by the substitution at the C5 atom, i.e. at 969.8 cm^{-1} in 5-FU, at 972.9 cm^{-1} in 5-ClU, at 973.6 cm^{-1} in 5-BrU and at 974.3 cm^{-1} in 5-IU. The experimental IR bands are localized at wavenumbers almost identical with those predicted by calculations. The IR and Raman intensity of the band is weak.

Mode 12 is predicted to occur at 760 ± 10 cm^{-1}. The calculations indicate that its IR intensity should be very weak or almost null while the Raman intensity is expected to be strong. In 5-IU it was calculated at 770.9 cm^{-1} in accordance with the Raman band observed at 750 cm^{-1}.

4.2.4.2. In-plane bending modes.
Corresponding to the modes nos. 16, 7, 6 and 5. Mode no. 16 appears slightly coupled with the $\nu(C5-X)$ mode. In uracil molecule it was computed at 987.7 cm^{-1}, but in 5-ClU it appears at 1079.4 cm^{-1}, in 5-BrU at 1052.7 and in 5-IU at 1033.8 cm^{-1}. Such wavenumber shifts are probably due to a significant contribution of the $\nu(C5-X)$ local mode. It is assigned in Ar matrix [33] at 1070, 1040 and 1020 cm^{-1} for 5-ClU, 5-BrU and 5-IU molecules, respectively. The band is of medium IR intensity, except for U for which it is rather weak. The Raman activity is predicted to be weak. Because of the small intensity of the band in U its assignment can be questioned. Only two papers have mentioned the ring bendings of 5-XU [33,55].

Mode 7 couples strongly with the $\nu(C-X)$ vibration, except in 5-IU with a weak coupling. For this reason, its wavenumber remarkably shifts to lower values with the increase of the halogen mass. Thus it was calculated at 741.7, 660.2, 625.3 and 609.5 cm^{-1} for the 5-FU, 5-ClU, 5-BrU and 5-IU molecules, respectively, in accordance to the Ar matrix [33] values at 652.5 (5-ClU), 623.0 (5-BrU) and 607.5 cm^{-1} (5-IU), whereas for the U molecule, for which it is practically uncoupled with other local modes, it is located at 556.0 cm^{-1}. This mode is of medium IR intensity, except for 5-FU where it is much weaker. The Raman activity is predicted to be very weak or almost null.

Mode 6 is calculated to occur at 586.8 cm^{-1} (scaled at 595.0 cm^{-1}) in accordance to the IR band observed at 598 cm^{-1}. The calculated intensity of the IR absorption is very weak, whereas the calculated activity of Raman scattering is medium and more or less constant from 5-FU to 5-IU molecule.

Mode 5 is little affected by halogen substitution. Thus it was calculated at 535.0, 536.1, 534.7 and 534.0 cm^{-1} for the 5-FU, 5-ClU, 5-BrU and 5-IU molecules, respectively. The scaled value at 545.0 cm^{-1} in 5-IU is in good accordance to the IR bands detected in the solid state at 540 and at 543 cm^{-1}.

4.2.4.3. Out-of-plane bending modes.
Of the three modes (nos. 1, 2 and 4) predicted to occur below 400 cm^{-1}, only mode 4 is predicted to appear in the IR spectra, and it should be placed between 360 and 420 cm^{-1}, with a low intensity, and contribute somewhat the $\gamma(C4=O)$ mode.

4.2.5. N–H modes
4.2.5.1. Stretching modes.
In the crystals of 5-IU, in the N–H stretching region exhibits a very broad band originated from the hydrogen-bonded network, which cannot be simply interpreted. Because in Ar matrix do not exist hydrogen bonds between the 5-IU molecules, the values reported by Zwierzchowska et al. [30] and Dobrowolski et al. [33] were selected as reference for the comparisons with the theoretical ones.

The calculations predicted the two stretching N–H bands to occur within the range 3450–3500 cm^{-1} and the N–H oscillators to be uncoupled. The v(N1–H) band is estimated to occur at wavenumber ca. 40 cm^{-1} higher than that of the v(N3–H) band. According to the harmonic wavenumber calculations, as the halogen mass is increased, the N1–H band shifts slightly towards lower wavenumbers, from 3629.5 cm^{-1} in 5-FU to 3621.1 cm^{-1} in 5-IU, while the N3–H band remains unshifted at 3585 cm^{-1}. The v(N–H) band separation is likely to slightly decrease from 5-FU (43 cm^{-1}) to 5-IU (37 cm^{-1}). In uracil the separation is 39 cm^{-1}.

In 5-IU the scaled values at 3469.2 and 3434.4 cm^{-1}, corresponding to the v(N1–H) and v(N3–H) modes, respectively, are in accordance to the experimental IR bands observed at 3470.0 and 3426.0 cm^{-1}, respectively, beyond any doubt. The intensity of the v(N1–H) band is calculated to be ca. 1.5 times higher than that of the v(N3–H) band, Fig. 4.

4.2.5.2. In-plane bending modes. According to the calculations, δ(N–H) mode appears strongly coupled with v(C–N) modes and form a complicated spectral pattern. All the modes in the 950–1500 cm^{-1} range have significant contributions due to δ(N–H) bending vibrations. The main contributions correspond to modes no. 23, a δ(N1–H), and no. 20a, δ(N3–H), positioned at 1487.4 and 1397.5 cm^{-1}, respectively (Table 3). As the halogen mass is increased, the δ(N1–H) mode wavenumbers are predicted to decrease slightly, from 1503.5 cm^{-1} in 5-FU, 1492.1 cm^{-1} in 5-ClU, 1489.2 cm^{-1} in 5-BrU, to 1487.4 cm^{-1} in 5-IU. In uracil it was computed at 1502.1 cm^{-1}. However, the δ(N3–H) mode remains almost unchanged, from 1401 cm^{-1} in 5-FU to 1397 cm^{-1} in 5-IU. The scaled values at 1448.1 (N1–H) and 1362.9 cm^{-1} (N3–H) in 5-IU are in accordance to the experimental IR values in Ar matrix at 1453 and 1384 cm^{-1}. Our assignment is in agreement with most of the literature data [54,57,58].

The IR intensities of the δ(N1–H) and δ(N3–H) modes tend to increase from 5-FU to 5-IU, but the increment is higher in δ(N3–H) than in δ(N1–H). As a consequence, in 5-FU the intensity of the δ(N1–H) mode is ca. 3 times greater than that of the δ(N3–H) mode, while in 5-IU it is only ca. 1.5 times.

The Raman activity of the δ(N1–H) mode tends to increase as the substituent mass is increased, while the Raman activity of the δ(N3–H) mode tends to decrease. As a consequence, in 5-FU the Raman activity of the δ(N1–H) mode is ca. 5 times greater than that of the δ(N3–H) mode, while in 5-IU it is ca. 20 times.

4.2.5.3. Out-of-plane bending modes. The out-of-plane bending mode, γ(N3–H) mode no. 9 is predicted to occur at 663.9 cm^{-1} (scaled at 668.0 cm^{-1}) in great accordance to the IR band observed in the solid state at 669 cm^{-1}, Table 4. The mode is nearly pure with PED of 75% and coupled with the γ(N1–H) mode. Its IR intensity is medium-strong and it increases slightly on passing from 5-FU to 5-IU. Its Raman activity is weak and is also predicted to increase slightly on passing from 5-FU to 5-IU.

The γ(N1–H) mode no. 8 is also predicted nearly pure with PED of 75% and coupled with the γ(N3–H) mode. It is calculated at 547.3 cm^{-1} (scaled at 557.6 cm^{-1}) in great accordance to the IR band observed in the solid state at 551 cm^{-1}. A slight increase in the calculated wavenumber of this mode is observed on passing from 5-FU at 526.5 cm^{-1} to 5-IU at 547.3 cm^{-1}. The calculated IR intensity of the mode is medium and slightly decreases from 5-FU to 5-IU while the calculated Raman activity is constant and almost nule.

In the experimental Raman spectrum several lines appeared below 200 cm^{-1}, which have been assigned [29] as C=O⋯H–N lattice vibrations.

4.2.6. C6–H modes

4.2.6.1. Stretching mode. The stretching mode, v(C6–H) mode no. 27 is predicted almost pure at 3235.6 cm^{-1} (scaled at 3104.0 cm^{-1}) in great accordance to the IR band observed experimentally in the solid state at 3106 cm^{-1}. However, Dobrosz-Teperek et al. [31] detected two bands, one more intense at 3086 cm^{-1} and another much weaker at 3056 cm^{-1}. The calculations predict that, as the substituent mass at position C5 is increased, the v(C6–H) band shifts toward lower wavenumbers, from 3244.2 cm^{-1} in 5-FU to 3235.6 cm^{-1} in 5-IU. Its IR intensity is very weak and also decreases from 5-FU to 5-IU. May be due to this weak IR intensity Dobrowolski et al. [33] did not observe the experimental band in Ar matrix. The Raman activity of this mode is very strong and also decreases from 5-FU to 5-IU.

4.2.6.2. In-plane bending mode. The δ(C6–H) mode no. 22 is calculated at 1350.2 cm^{-1} (scaled at 1318.1 cm^{-1}) in a good agreement with the IR band observed experimentally in the solid state at 1323 cm^{-1}. This mode is strongly coupled with C=C, C–N and N1–H bending modes. The analogous band in uracil is predicted to occur at 1381.4 cm^{-1} (calculated at 1417.0 cm^{-1}) in accordance to the IR band in gas-phase [58] at 1396 cm^{-1}, and to be coupled with N–H and C–N ring modes. The theoretical IR intensity of this mode changes irregularly while the Raman activity is expected to decrease slightly as the halogen mass is increased.

4.2.6.3. Out-of-plane bending mode. The γ(C6–H) mode no. 15 is predicted to occur in the range of 875–925 cm^{-1} and to increase on passing from 5-FU to 5-IU, whereas for uracil molecule it is predicted to occur at ca. 970 cm^{-1}. In 5-IU it was calculated at 917.9 cm^{-1} (scaled at 908.6 cm^{-1}) as an almost pure mode (95% PED), in accordance to the IR band observed in the solid state [29] at 910 cm^{-1} and in Ar matrix [33] at 904.0 cm^{-1}. The theoretical IR intensity of the mode is weak and decreases on passing from 5FU to 5-IU, while for U this mode is predicted to be almost inactive. The Raman activity of the mode is very weak and thus it was not detected in the experimental Raman spectrum.

4.2.7. C–I modes

4.2.7.1. Stretching modes. In $H_2NC(=O)CH_2I$ the stretching v(C–I) mode has been reported [59] at 465 cm^{-1}, in CH_2I_2 at 485 cm^{-1}, and in $HOC(=O)CH_2I$ at 635 cm^{-1}. However in 5-IU it was calculated at 238.5 cm^{-1} (scaled at 265.1 cm^{-1}). The low wavenumber prediction for this mode with our theoretical methods appears as a contradiction with the spectral region of 560 ± 100 cm^{-1} reported [59] for other compounds with iodine. It can be tentatively explained by the fact that when a halogen atom is directly attached to a ring, the C–X stretch vibration tends to interact with the ring vibrations [60] and can leads to a remarkable reduction in its wavenumber, as in the present case with 5-IU.

The calculated IR intensity is almost nule and thus it was not detected in the experimental IR spectra. By contrast, the Raman band shows an appreciable intensity and it was detected at 245 cm^{-1}.

4.2.7.2. In-plane bending modes. The in-plane bending, δ(C–I) deformation appears coupled (20% PED) with a ring mode, and it is predicted at 156.8 cm^{-1} (scaled at 187.7 cm^{-1}) in accordance with the bibliography [60], 220 ± 100 cm^{-1}. The theoretical prediction of δ(C5–X) bending vibrations show a systematic decrease on passing from 5-FU to 5-IU molecule. The theoretical IR intensity of the δ(C5–X) mode increases, and the Raman activity decreases from 5-ClU to 5-IU.

4.2.7.3. Out-of-plane bending modes. The out-of-plane bending mode γ(C5–X) appear strongly coupled with C=O and ring modes

and are predicted to decrease significantly its position with the halogen atom mass from 112.8 cm^{-1} in 5-FU to 80.5 cm^{-1} in 5-IU. This mode is practically IR inactive, decreasing its intensity from 5-FU to 5-IU. Analogously its Raman activity, except in 5-BrU which appears with medium intensity.

5. Other molecular properties

Calculated wavenumbers have been employed, along with the corresponding theoretical equilibrium geometries, to yield thermodynamic properties of 5-IU. The values of the natural charges obtained with the theoretical methods used are listed in Table 5. Small changes have been observed between 5-IU and uracil molecule. As it is expected, the largest changes in the charge occur on the X11 and C5 atoms, then on the two carbons atoms neighboring to C5 atom, and next on the H12 and O10 atoms. Finally the change of charge is almost negligible for the atoms most distanced from the X11 atom.

The calculated thermodynamic parameters are collected in Table 6. The theoretical data are employed to correct experimental thermochemical information at 0 K, as well as for the effect of the zero-point vibrational energy (ZPVE). In the ZPVE, scaling factors of 0.89 and 0.93 have been recommended to be used [61] with HF to improve their know overestimation. Several thermodynamic parameters such as enthalpy, heat capacity, free energy and entro-py have been calculated in 5-IU from the vibrational frequencies obtained from the IR and Raman spectra [62].

The entropies calculated for several kinds of compounds at different *ab initio* levels have been reported [63] to be in agreement with the experimental data, with the mean absolute deviation less than 5%. The differences are attributed to the neglect of residual (orientation) entropy present at 0 K in the crystal.

In uracil molecule, the experimental dipole moment μ of tautomer U1 is known: 4.13 D in dioxane solution [64], 3.87 D in gas-phase [65] and 4.01 ± 0.02 D in book's Tables [66]. Our calculated value at the B3LYP/6-311++G(3df,pd) level, 4.481 D, is in reasonable agreement with these results by considering that the reported experimental data to be accurate to ±10%. The increase of the basis set of DFT method has little effect on this parameter.

In 5-IU molecule the calculated dipole moment μ at the B3LYP/DGDZVP level in tautomer U1 is slightly lower than in uracil molecule, 4.55 D (Table 6), as in the other 5-halosubstituted uracils.

5.1. Tautomerism

Due to the feasible relationship between the occurrence of the rare enol tautomeric forms of uracil and point mutations developing during RNA replications, numerous studies have been reported. From these studies a large amount of work has been performed on the tautomerism of nucleic acid bases, using both theoretical [67–69] and experimental [70–72] approaches. Much of the interest is due to the fact that tautomers induce alterations in the normal base pairing, leading to the possibility of spontaneous mutations in the DNA or RNA helices. Tautomerism in nucleic acid bases have a role in mutagenesis of DNA. The process is intimately connected with the energetics of the chemical bonds.

The *uracil molecule* may exist in various tautomeric forms differing from each other by the position of the proton, which may be bound to either ring nitrogen atoms or oxygen atoms. Proton migration causes expected sizeable variations in the ring structure and the exocyclic CO bond lengths. It has been recently studied that the proton transfer proceeds from isolated U to uracil tautomer (UT) via a transition state (Uts) [73]. The process has been reported to be difficult, with a high barrier of 42.75 kcal/mol. Of all the possible combinations, six uracil tautomers, named U1–U6, are the most important and studied tautomers [74]. The most stable one, the dioxo form **U1**, is the only one for which experimental information is available, Table 7. Our calculated values in uracil molecule confirm the stability of form U1, which is in agreement with the experimental results [75] and with previous *ab initio* cal-

Table 5
Calculated natural total atomic charges on the atoms in 5-IU and uracil molecules.

Atoms	5-IU		Uracil		
	HF/3-21G**[a]	B3LYP/DGDZVP	HF/3-21G**[a]	B3LYP/DGDZVP	B3LYP/6-311++G (3df,pd)
N1	−0.91	−0.65	−0.91	−0.66	−0.61
C2	1.22	0.91	1.21	0.91	0.82
N3	−0.95	−0.7	−0.95	−0.7	−0.64
C4	0.94	0.71	0.91	0.72	0.65
C5	−0.48	−0.39	−0.36	−0.37	−0.36
C6	0.36	0.08	0.33	0.09	0.08
H7	0.3	0.44	0.3	0.43	0.42
O8	−0.62	−0.67	−0.63	−0.67	−0.63
H9	0.31	0.44	0.31	0.44	0.42
O10	−0.59	−0.62	−0.62	−0.64	−0.6
I	0.19	0.22	0.19[b]	0.24[b]	0.24[b]
H12	0.22	0.23	0.21	0.22	0.21

[a] Mulliken charges.
[b] With H11.

Table 6
Theoretical computed heat of formation, zero-point vibrational energies, rotational constants, entropies and dipole moments in 5-IU and uracil molecules.

Parameters	5-IU		Uracil		
	HF/3-21G**	B3LYP/DGDZVP	HF/3-21G**	B3LYP/DGDZVP	B3LYP/6-311++G (3df,pd)
Total energy + ZPE (AU)	.42410[a]	.05246[b]	.09587[c]	.79039[d]	.88882[d]
Zero-point energy (KJ/mol)	53.14	200.25	60.21	227.68	228.08
Rotational constants (GHz)	3.02	2.94	3.93	3.86	3.9
	0.49	0.48	2.04	2	2.02
	0.42	0.41	1.34	1.32	1.33
Entropy (cal·mol^{-1}·K^{-1})					
Total	88.02	91.41	76.52	79.34	79.03
Translational	42.3	42.3	40.06	40.06	40.06
Rotational	30.63	30.69	27.79	27.85	27.81
Vibrational	15.09	18.42	8.67	11.43	11.16
Dipole moments (Debyes)	4.31	4.06	4.79	4.55	4.48

[a] −7297.
[b] −7334.
[c] −410.
[d] −414.

Table 7
Gas-phase relative energies (Kcal/mol) of uracil and 5-IU tautomers.

Method	U1	U2	U3 (U3b)	U4 (U4b)	U5	U6	U7	U8	U9	U10
Uracil										
B3LYP/6-311++G(3df,pd) + ZPE	0.00	11.12	11.53	12.89	18.89	20.34				
B3LYP/DGDZVP + ZPE	0.00	11.68	12.76	14.47	20.12	21.63				
B97-1/6-311+G(2d,p)	0.00	10.93	11.35	12.13	18.97	20.7				
/cc-pVDZ + ZPE	0.00	11.4	12.47	13.15	20.55	21.37				
/aug-cc-pVDZ + ZPE	0.00	10.7	11.19	11.93	18.65	19.78				
CCSD/6-31G** [78]	0.00	11.19	12.88	12.39	19.62	22.6				
Experimental, Ref. [81]					19 ± 6	22 ± 10				
5-IU										
B3LYP/DGDZVP + ZPE	0.00	10.46	13.09 (17.98)	13.57 (16.67)	18.74	18.82	79.03	70.05	90.04	75.82

culations [76]. U1 is predicted to be the only tautomer present in the vapour, although fluorescence studies seem to suggest that a fraction of the keto-enol tautomer could exist [77]. Generally, the keto form of uracil exists as the main form in the double helix. The formation of specific AU Watson–Crick hydrogen bonds is responsible for the maintenance of the genetic code. If uracil is replaced by another type of base, it may lead to the introduction of a wrong genetic code.

Solvent interactions partly modify the gas-phase order of stability of the tautomers. The U1 di-oxo form remains the most stable structure while the relative stability of the keto-enolic U2 and U3 forms is reversed. The relative stabilities of U2, U3 and U4 in acetonitrile solution are found [78] to be 12.2, 10.3 and 14.9 kcal/mol, and 11.5, 11.0 and 13.4 kcal/mol, in carbon tetrachloride, compared to the gas-phase values of 10.9, 11.3 and 12.0 kcal/mol, respectively. Similar results were reported [79,80] with the Onsager's SCRF model.

Following the same methodology as that with uracil molecule, in **5-IU** was determined, in principle, 10 tautomers, Fig. 1. The tautomers appear plotted in the optimum form optimized at the B3LYP/DGDZVP level. Using the same notation as in reference [74], tautomers U1–U6 correspond to that of uracil, while due to the iodine atom tautomers U7–U10 are only characteristic of 5-IU. The gas-phase relative energies of 5-IU tautomers are shown in Table 7, which can be compared with those corresponding to uracil molecule. Unfortunately there are not studies on 5-IU molecule to compare our results, but the accordance found with our calculated data in uracil molecule with the DGDZVP basis set with those of the sophisticated CCSD/6-31G* basis, with differences lower than 1 kcal/mol, permit us to assume that the calculated values on 5-IU molecule are satisfactory. Only the calculated energy with U4 tautomer differs slightly with a difference of ca. 2 kcal/mol.

The relative stabilities of the tautomers have been found to be somewhat sensitive to both the basis set and the theoretical method used, showing variations within 1.5 kcal/mol. The zero-point energy (ZPE) contribution also shows this sensitivity, with variations 0.2–0.7 kcal/mol (2–3%). Both basis set and ZPE corrections do not change the order of stability of the tautomers.

As in uracil molecule, the dioxo form **U1** of 5-IU molecule is the most stable one. It was the tautomer discussed in the previous sections of the present paper.

The next most stable tautomer is the keto-enolic form **U2**, 10.5 kcal/mol above U1 in 5-IU and 11.7 kcal/mol above U1 in uracil at the B3LYP/DGDZVP level, Table 7. The calculated value at this level is very close to that reported at the sophisticated CCSD/6-31G** level [78], 11.19 kcal/mol.

As compared with U1, the main effect with the displacement of the proton on N1 is a large shortening in U2 of the N1–C2 bond, 1.302 Å vs. 1.394 Å of U1, as well as shortening of the N1–C6, C2–N3, C4–C5 bonds and lengthening of the C2–O, N3–C4, C5–C6 bonds. The small largening of the C5–I bond (2.110 Å vs. 2.106 Å

in U1) is counteract with a closening of the C4–C5–I angle (117.7° vs. 118.4° of U1). The *tilt* angle ε (Fig. 2) is slightly increased, 2.2° vs. 1.7 in U1. The proton of the hydroxy group remains in the ring plane, with a N1–C2–O7–H12 torsional angle of −0.04°.

Tautomers **U3**–**U4** are the next most stable ones. They are very close in energy, ca. 0.5 kcal/mol. Tautomer U3 appears more stable than U4 in accordance with that found in uracil molecule (except at the CCSD/6-31G** level, Table 7).

The formation of the O–H12 group in these tautomers leads to a closening of the N3–C4=O angle (118.0° in U3 and 117.5° in U4 vs. 120.3° in U1) due to a weak N3···H12 attraction (ca. 2.24 Å). This fact leads to a remarkable opening of the N3–C4–C5 angle (124.7° in U3 and 122.3° in U4 vs. 113.2° in U1) and a closening of the C5–C4=O angle (117.3° in U3 and 120.2° vs. 126.5° in U1). It leads to a shortening of the intramolecular distance between the iodine atom and the neighbor oxygen of the carbonyl group; O···I is 3.261 Å in U3 and 3.282 Å in U4 vs. 3.317 Å of U1, and a lengthening of the C5–I bond 2.112 Å in U3 and 2.114 Å in U4 vs. 2.106 Å of U1. The closening of the C5–C4–O angle leads to an increase of the deformation of the angles on the iodine atom with C4–C5–I angle (123.2° in U3, 122.6° in U4 vs. 118.4° in U1) and a closing of the *ipso* angle C4–C5=C6 (115.2° in U3, 115.6 in U4 vs. 119.7° in U1), while the C6=C5–I angle remains almost unchanged (121.6° in U3, 121.8° in U4 vs. 121.9° in U1). The *tilt* angle is very low, 0.8° in U3 and 0.4° in U4.

In the hydroxy form, the negative charge on the oxygen bonded to C4 atom is slightly increased (up to ca. −0.700 vs. −0.625 in U1) and −0.640 in U2, but it does not affect to the positive charge on the iodine atom. Thus, it is 0.205 in U3 with the OH12 group which is very close to 0.204 in U2 with a C4=O group.

With an OH group appearing bonded on C4, the hydrogen atom can be in *trans* position related to the iodine atom (tautomers U3, U4 and U9) or in *cis* position (tautomers U3b, U4b and U6). In both cases a shortening of the N3–C4 (and N1–C6) bonds is observed, ca. 0.1 Å in tautomers U3, U4 and U9, and ca. 0.06 Å in tautomer U6. This shortening increase the quinonoid character of the ring, with an opening of the N1–C4–C5 angle, ca 10° in the tautomers U3, U4 and U9, and ca. 5° in tautomer U6. This less change in the parameters in the tautomer U6 is also observed on the closening of the C4–C5–C6 angle, ca. 4° in tautomers U3, U4, and ca. 3° in tautomer U6.

Tautomer **U5** appears in uracil molecule 6 kcal/mol less stable than U4, while in 5-IU molecule, the difference is ca. 5 kcal/mol. It is curious that this tautomer is less stable than U4, when in last one two protons are migrated. Perhaps U4 appears stabilized because the uracil ring shows high aromaticity with alternated double bonds, Fig. 1. Thus, the N1–C2, N3–C4, C5–C6 bonds are shorter than N1–C6, C2–N3, C4–C5.

It is also noted that U5 is also less stable than U2, when N1–H bond is 0.004 Å shorter than N3–H and when the force constant of N1–H is 0.18 mDyne/Å higher than N3–H. Perhaps it is due to

some electronic delocalisation in the uracil ring of U2 which stabilizes this tautomer vs. U5 with high quinonoid character of the uracil ring and thus high dipole moment, 6.74 D vs. 4.16 of U2.

Tautomer **U6** appears with almost the same stability than U5 (the difference is only 0.08 kcal/mol), although in uracil molecule the difference is 1.5 kcal/mol. The less stability of this form is due to the proton on N1 needs to move to the other side of the molecule to be placed on O9. The placement of this proton can be in *syn* position regarding the iodine atom, or in *trans* position (a saddle form). In the first case, tautomer U6, the repulsion of H12 with the iodine atom leads to a reduction in the deformation of the angles involving the iodine atom, i.e. C4–C5–I and C6=C5–I, 120.8° and 122.8°, respectively, while in tautomer U1 are, 118.4° and 121.9°, respectively. It is noted in all the tautomers that the C4–C5–I angle is always lower, ca. 4°, than the C6=C5–I angle, except in the U3 and U4 tautomers with an OH group bonded to C4. In this last case the C6=C5–I angle is ca. 1–2° higher than the C4–C5–I angle.

The negative charge on O9 in this *syn* form, −0.700, remains almost unchanged as compared with U3 and U4 tautomers where the hydrogen is in *trans* form. However, the positive charge on the iodine atom, 0.174, appears slightly reduced, 0.194 in U4 and 0.205 in U3.

Tautomers **U7–U10** corresponding to the migration of the amino hydrogen to the iodine atom are much less stable than U1–U6. This hydrogen is placed in *trans* form with regard to the C4=O group. The *cis* form is not stable. In tautomers U7 and U8 one hydrogen appears migrated, while in tautomers U9 and U10 two hydrogens are migrated. These tautomers are planar, with the exception of tautomer U9, and the C5–I–H12 angle is ca. 94.5°.

Tautomer **U8** is 9 kcal/mol more stable than U7 due to a lower value of the *tilt* angle ε, 17.5° in U8 vs. 19.3° in U7. The migration of the hydrogen bonded to N1 leads to a tautomer more stable than when the migration is with the hydrogen bonded to N3 (tautomer U7). This fact has been also observed between tautomers U2 and U3, being tautomer U2 more stable than U3. The ε' angle is also lower in U8 than in U7, 3.3° vs. 4.9° in U7.

Tautomer **U9** is the only one that appears with the hydrogen on the iodine atom out-of ring plane, Figs. 1 and 3. The C4–C5–I–H12 is 85.1°. Because in the planar form this H12 hydrogen is repulsed by the H10 hydrogen on C6 and by the OH group bonded to C4, while in the other tautomers only the oxygen atom appears bonded to C4. Due to this repulsion, the C5–I–H12 angle is remarkably opened (115.9° vs. 94.6° in U7 and 94.3° in U8) as well as the C4–C5–I angle (121.6 in U9 vs. 99.2° in U7 and 100.8° in U8), and this tautomer has the lowest stability out of the ten studied tautomers.

In this tautomer the uracil ring also appears deformed, with a C4–C5–C6–N1 of 4.51°, N3–C4–C5–C6 of −4.59°, N1–C2–N3–C4 of 3.40° and N3–C2–N1–C6 of −3.47°. The sum of the angles around C5 is 119.7°.

Tautomer **U10** is more stable than U7, ca. 3 kcal/mol, but ca. 6 kcal/mol less stable than U8. Perhaps it is due to the fact that when the two amino hydrogens are migrated, the ε angle is lower than U7, but ca. 1° higher than U8.

It is noted in all these tautomers the N1–C2=O angle is lower than the N3–C2=O, between 1° and 8°, except in tautomers U2, U4, U6 and U8 with an hydroxy group bounded to C4.

5.2. Dipole moments

The prediction of accurate dipole moments is a very important issue, because the magnitude of the dipole moment is strongly related to the tautomeric stability in polar environments. Different tautomers have different electronic structures and, in principle, may display significant variations in their physical properties.

Table 8
Dipole moments (μ, debye), of uracil and 5-IU tautomers.

Tautomer	Uracil			5-IU
	B97-1[a]	B3LYP[b]	B3LYP[c]	B3LYP[c]
U1	4.49	4.48	4.55	4.06
U2	3.27	3.33	3.36	4.16
U3	4.92	4.88	4.91	3.8
U4	1.24	1.18	1.24	0.59
U5	6.56	6.58	6.58	6.74
U6	7.16	7.2	7.35	6.05
U7	–	–	–	11.34
U8	–	–	–	9.41
U9	–	–	–	11.85
U10	–	–	–	7.76

[a] At the B97-1/d-aug-cc-pVDZ level, Ref. [78].
[b] At the B3LYP/6-311++G(3df,pd) level.
[c] At the B3LYP/DGDZVP level.

In the first six tautomers of 5-IU which are analogues to uracil, the calculated μ lies in a wide range of values ($1 - 7$ D), Table 8, increasing in the order U4 < U2 < U1 < U3 < U5 < U6 in uracil molecule, and in the order U4 < U3 < U1 < U2 $\leqslant$ U6 < U5 in 5-IU. This order remains with the change of basis set of DFT method. In 5-IU molecule it is noted that tautomers U2 and U3, and tautomers U5 and U6 appear in reverse order as compared to those of uracil. It is due to the close dipole moment values.

Tautomers U7–U10 have larger μ than U1–U6, and they are in the range of values 7–12 D. The less stable tautomer U9 in gas-phase has the largest μ, i.e. it is the most stable in solution.

6. Summary and conclusions

The most important findings of this study are the following:

(1) With the purpose of study of the 5-IU molecule, its equilibrium geometries and harmonic wavenumbers were calculated at various DFT levels. The computed vibrational values appear reasonable when they are compared with IR and Raman experimental data. An accurate assignment was performed in 5-IU molecule according to the notation of the uracil normal modes.

(2) To improve the calculated wavenumbers, two procedures for scaling the values were used. The specific scale factor procedure gives rise to a slightly more noticeable improvement in the predicted wavenumbers, than when the scaling equation was used. Although for its simplicity, second procedure is recommended for the scaling. The mean deviation after scaling is ca.10 cm^{-1}.

(3) The accuracy obtained with semiempirical methods is slightly lower than with DFT methods, but they are computationally less expensive.

(4) The values of the total atomic charges, the dipole moments, and the other thermodynamic parameters were also coherent.

(5) Ten tautomeric forms of 5-IU were determined and optimized. Six of them are related to those of uracil molecule, with the same stability order.

References

[1] S.M. Morris, Mutat. Res. 297 (1993) 39.
[2] S.D. Soni, T. Srikrishnan, J.L. Alderfer, Nucleosides Nucleotides 15 (1996) 1945.
[3] G. Tunnicliff, T.L. Youngs, Biochem. Arch. 13 (1997) 37.
[4] (a) C.A. Presant, W. Wolf, V. Waluch, C. Wiseman, P. Kennedy, D. Blayney, R.R. Brechner, Lancet 343 (1994) 1184;
(b) T. Nakajima, World J. Surg. 19 (1995) 570.
[5] (a) W.C. Chu, A. Klintanar, J. Horowitz, J. Mol. Biol. 227 (1992) 1173;
(b) W.C. Chu, V. Feiz, W.B. Derrick, J. Horowitz, J. Mol. Biol. 227 (1992) 1164.
[6] (a) I. Verheggen, A. van Aerschot, L. van Meervelt, J. Rozenski, L. Wiebe, R. Snoeck, G. Andrei, J. Balzarini, P. Claes, E. De Clercq, J. Med. Chem. 38 (1995) 826;
(b) H.O. Kim, S.K. Ahn, A.J. Alves, J.W. Beach, L.S. Jeong, B.G. Choi, P. van Roey, R.F. Scinazi, C.K. Chu, J. Med. Chem. 35 (1992) 1987.
[7] (a) B.A. Katzung (Ed.), Basic and Clinical Pharmacology, sixth ed., Appleton & Lange, Norwalk, CT, 1995;
(b) H.O. Kim, S.K. Ahn, A.I. Alves, I.W. Beach, J. Med. Chem. 35 (1992) 1987.
[8] Y. Yoshimura, K. Kitano, K. Yamada, S. Sakata, S. Miura, N. Ashida, H. Machida, Bioorg. Med. Chem. 8 (2000) 1545.
[9] Z.B. Yang, M.T. Rodgers, J. Am. Chem. Soc. 126 (2004) 16217.
[10] Elisenda Ferrer, Marten Wiersma, Bernard Kazimierczak, Christoph W. Mueller, Ramon Eritja, Bioconjug. Chem. 8 (1997) 757.
[11] A. Rochdi, M. Taourirte, N. Redwane, H.B. Lazrek, J.L. Barascut, J.L. Imbach, Nucleosides Nucleotides 18 (1999) 673.
[12] T. Oyoshi, A.H.J. Wang, H. Sugiyama, J. Am. Chem. Soc. 124 (2002) 2086.
[13] V.K. Rastogi, V. Jain, R.A. Yadav, C. Singh, M. Alcolea Palafox, J. Raman Spectrosc. 31 (2000) 595.
[14] V.K. Rastogi, M. Alcolea Palafox, L. Mittal, N. Peica, W. Kiefer, K. Lang, S.P. Ojha, J. Raman Spectrosc. 38 (2007) 1227.
[15] (a) C. Singh, M. Alcolea Palafox, N.P. Bali, S.S. Bagchi, P.K. Shrivastava, Asian Chem. Lett. 3 (1999) 248;
(b) M. Alcolea Palafox, G. Tardajos, A. Guerrero-Martínez, V.K. Rastogi, D. Mishra, S.P. Ojha, W. Kiefer, Chem. Phys. 340 (2007) 17;
(c) M. Alcolea Palafox, O.F. Nielsen, K. Lang, P. Garg, V.K. Rastogi, Asian Chem. Lett. 8 (2004) 81.
[16] L. Deng, S. Shuman, J. Biol. Chem. 272 (1997) 695.
[17] (a) K.M. Meisenheimer, T.H. Koch, Crit. Rev. Biochem. Mol. Biol. 32 (1997) 101;
(b) D.L. Wong, J.G. Pavlovich, N.O. Reich, Nucleic Acids Res. 26 (1998) 645;
(c) A. Jeltsch, M. Roth, T. Friedrich, J. Mol. Biol. 285 (1999) 1121;
(d) B. Holz, N. Dank, J.E. Eickhoff, G. Lipps, G. Krauss, E. Weinhold, J. Biol. Chem. 274 (1999) 15066;
(e) C.L. Norris, P.L. Meisenheimer, T.H. Koch, J. Am. Chem. Soc. 118 (1996) 5796;
(f) M.C. Willis, B.J. Hicke, O.C. Unlenbeck, T.R. Cech, T.H. Koch, Science 262 (1993) 1255.
[18] U.P. Singh, B.N. Singh, A.K. Ghose, R.K. Singh, A. Sodhi, J. Inorg. Biochem. 44 (1991) 277.
[19] D.W. Adair, K. A. Smiles, D. King, Eur Pat Appl EP 565412 A1, 1993, p. 51.
[20] I. Verheggen, A. Van Aerschot, L. Van Meervelt, J. Rozenski, L. Wiebe, R. Snoeck, G. Andrei, J. Balzarini, P. Claes, E. De Clercq, J. Med. Chem. 38 (1995) 826.
[21] (a) H.S. Randhawa, M.S. Jassal, B. Sirdhana, B.S. Sekhon, Ind. J. Chem. Sect. A 37 (1998) 517;
(b) C. Parkanyi, C. Boniface, J. J Aaron, M.D. Gaye, L. von Szentpaly, R. Ghosh, K.S. Raghu Veer, Struct. Chem. 3 (1992) 277;
(c) M. Monshi, K. Al-Farhan, A. Al-Resayes, A. Ghaith, A.A. Hasanein, Spectrochim. Acta 53A (1997) 2669.
[22] A.A. Hasanein, M.A. Morsy, J. Saudi Chem. Soc. 2 (1998) 35.
[23] G.C. Crittenden, O. Haugen, S. Prydz, Int. J. Radiat. Biol. 27 (1975) 447.
[24] B. Nagasaka, S. Takeda, N. Nakamura, Chem. Phys. Lett. 222 (1994) 486.
[25] E. Bednarek, J.C. Dobrowolski, K. Dobrosz-Teperek, L. Kozerski, W. Lewandowski, A.P. Mazurek, J. Mol. Struct. 554 (2000) 233.
[26] J. Witowska, J. Cz. Dobrowolski, K. Dóbrosz-Teperek, W. Lewandowski, A.P. Mazurek, 14th International Mass Spectrometry Conference, Tempere, Finland, 1997.
[27] M. Misra, R.F. Egerton, J. Microsc. 139 (1985) 197.
[28] S.C. Wait Jr., M. Sirota, J.C. Corelli, Radiat. Eff. 35 (1978) 79.
[29] (a) S. Kumar, S.K. Singhal, J.P. Goel, M. Srivastava, Asian J. Phys. 5 (1996) 247;
(b) V. Sharma, S.D. Sharma, Seema, B.S. Yadav, Asian J. Phys. 3 (1994) 229.
[30] Z. Zwierzchowska, K. Dobrosz-Teperek, W. Lewandowski, R. Kolos, K. Bajdor, J. Cz. Dobrowolski, A.P. Mazurek, J. Mol. Struct. 410 (1997) 415.
[31] K. Dobrosz-Teperek, Z. Zwierzchowska, W. Lewandowski, K. Bajdor, J. Cz. Dobrowolski, A.P. Mazurek, J. Mol. Struct. 471 (1998) 115.
[32] T. Ueda, K. Shinozaki, K. Ushizawa, A. Yimit, M. Tsuboi, Nucleic Acids Symp. Ser. 37 (1997) 95.
[33] J.Cz. Dobrowolski, J.E. Rode, R. Kolos, M.H. Jamróz, K. Bajdor, A.P. Mazurek, J. Phys. Chem. 109 (2005) 2167.
[34] M.J.S. Dewar, E.G. Zoebisch, E.F. Healy, J.J.P. Stewart, J. Am. Chem. Soc. 107 (1985) 3902.
[35] M.J.S. Dewar, C. Jie, J. Yu, Tetrahedron 49 (1993) 5003.
[36] A.J. Holder, AMPAC 5.0, 1994, Semichem Inc., 7128 Summit, Shawnee KS 66216, USA.
[37] N. Nakatsuji, M. Hada, M. Ehara, K. Toyota, R. Fukuda, J. Hasegawa, M. Ishida, T. Nakajima, Y. Honda, O. Kitao, H. Nakai, M. Klene, X. Li, J.E. Knox, H.P. Hratchian, J.B. Cross, C. Adamo, J. Jaramillo, R.E. Stratmann, O. Yazyev, A.J. Austin, C. Pomelli, J.W. Ochterski, K. Morokuma, G.A. Voth, P. Salvador, J.J. Dannenberg, S. Clifford, M.J. Frisch, G.W. Trucks, H.B. Schlegel, G.E. Scuseria, M.A. Robb, J.R. Cheeseman, V.G. Zakrzewski, J.A. Montgomery Jr., R.E. Stratmann, J.C. Burant, S. Dapprich, J.M. Millam, A.D. Daniels, K.N. Kudin, M.C. Strain, O. Farkas, J. Tomasi, V. Barone, M. Cossi, R. Cammi, B. Mennucci, C. Pomelli, C. Adamo, S. Clifford, J. Ochterski, G.A. Petersson, P.Y. Ayala, Q. Cui, K. Morokuma, D.K. Malick, A.D. Rabuck, K. Raghavachari, J.B. Foresman, J. Cioslowski, J.V. Ortiz, A.G. Baboul, B.B. Stefanov, G. Liu, A. Liashenko, P. Piskorz, I. Komaromi, R. Gomperts, R.L. Martin, D.J. Fox, T. Keith, M.A. Al-Laham, C.Y. Peng, A. Nanayakkara, M. Challacombe, P.M.W. Gill, B. Johnson, W. Chen, M.W. Wong, J.L. Andres, C. Gonzalez, M. Head-Gordon, E.S. Replogle, J.A. Pople, Gaussian 03, Revision B.04, Gaussian, Inc., Pittsburgh PA, 2003.
[38] (a) J.M. Seminario, P. Politzer (Eds.), Modern Density Functional Theory: A Tool for Chemistry, vol. 2, Elsevier, Amsterdam, 1995;
(b) A.D. Becke, J. Chem. Phys. 97 (1992) 9173. 98 (1993) 5648;
(c) C. Lee, W. Yang, R.G. Parr, Phys. Rev. B37 (1988) 785.
[39] (a) N. Godbout, D.R. Salahud, J. Andzelm, E. Wimmer, Can. J. Chem. 70 (1992) 560;
(b) C. Sosa, J. Andzelm, B.C. Elkin, E. Wimmer, K.D. Dobbs, D.A. Dixon, J. Phys. Chem. 96 (1992) 6630.
[40] T.R. Cundari, W.J. Stevens, J. Chem. Phys. 98 (1993) 5555.
[41] (a) T. Leininger, A. Nicklass, H. Stoll, M. Dolg, P. Schwerdtfeger, J. Chem. Phys. 105 (1996) 1052;
(b) X.Y. Cao, M. Dolg, J. Mol. Struct. (THEOCHEM) 581 (2002) 139.
[42] G. Ferenczy, L. Harsányi, B. Rozsondai, I. Hargittai, J. Mol. Struct. 140 (1986) 71.
[43] L. Harsányi, A. Császár, P. Császár, J. Mol. Struct. (THEOCHEM) 137 (1986) 207.
[44] R.F. Stewart, L.H. Jensen, Acta Crystallogr. 13 (1967) 1102.
[45] H.L. Meyerheim, T. Gloege, Phys. Status Solidi Appl. Res. 173 (1999) 175.
[46] D. Dobritzsch, S. Ricagno, G. Schneider, Klaus D. Schnackerz, Ylva Lindqvist, J. Biol. Chem., 277 (2002) 13155.
[47] H. Sternglanz, G.R. Freeman, C.E. Bugg, Acta Crystallogr. B31 (1975) 1393.
[48] A.D. Mitchell, A.E. Somerfield, L.C. Cross, Interatomic Distances Spec Publ. No. 18, 1965, The Chemical Society, Burlington House, London.
[49] (a) L. Fallon III, Acta Crystallogr. B29 (1973) 2549;
(b) H. Sternglanz, C.E. Bugg, Biochem. Biophys. Acta 1 (1975) 378.
[50] M. Alcolea Palafox, N. Iza, M. Gil, J. Mol. Struct. (THEOCHEM) 585 (2002) 69.
[51] (a) M. Alcolea Palafox, Recent Phys. Dev. Phys. Chem. 2 (1998) 213;
(b) M. Alcolea Palafox, Int. J. Quantum Chem. 77 (2000) 661.
[52] A.P. Scott, L. Radom, J. Phys. Chem. 100 (1996) 16502.
[53] H.P. Mital, S. Bhardwaj, S.K. Singhal, R.K. Sharma, Asian Chem. Lett. 1 (1997) 77.
[54] M.J. Nowak, Nucleic Acid Bases Isolated in Gaseous Matrixes, Dissertation, Instytut Fizyki PAN, Warszawa, Poland, 1993.
[55] M. Graindourze, T. Grootaers, J. Smets, Th. Zeegers-Huyskens, G. Maes, J. Mol. Struct. 237 (1990) 389.
[56] S.G. Stepanian, E.D. Radchenko, G.G. Sheina, Y.P. Blagoi, Biofizika 34 (1989) 753.
[57] K. Szczepaniak, W.B. Person, J. Leszczynski, J.S. Kwiatkowski, Pol. J. Chem. 72 (1998) 402.
[58] Yu. Ivanov, A.M. Plokhotnichenko, E.D. Radchenko, G.G. Sheina, Yu.P. Blagoi, J. Mol. Struct. 372 (1995) 91.
[59] D. Lin-Vien, N.B. Colthup, W.G. Fateley, J.G. Grasselli, The Handbook of Infrared and Raman Characteristic Frequency of Organic Molecules, Academic Press, San Diego, California, USA, 1991.
[60] N.P.G. Roeges, A guide to the complete interpretation of Infrared spectra of organic structures, John Wiley & Sons, New York, 1994.
[61] (a) J.A. Pople, H.B. Schlegel, R. Krishnan, D.J. Defrees, J.S. Binkley, M.J. Frisch, R.A. Whiteside, Int. J. Quantum Chem. Symp. 15 (1981) 269;
(b) H.B. Schlegel, J. Phys. Chem. 88 (1984) 6254.
[62] S.K. Singhal, V.P. Arora, Y.C. Sharma, Asian Chem. Lett. 3 (1999) 48.
[63] (a) W.J. Hehre, L. Radom, P.V.R. Schleyer, J.A. Pople, Ab Initio Molecular Orbital Theory, Wiley, New York, 1986;
(b) G. Leroy, M. Sana, C. Wilante, D.R. Temsamani, J. Mol. Struct. (THEOCHEM) 259 (1992) 369;
(c) M. Sana, G. Leroy, Theor. Chim. Acta 77 (1990) 383.
[64] I. Kulakowska, M. Geller, B. Lesyng, K.L. Wierzchowski, K. Bolewska, Biochim. Biophys. Acta 407 (1975) 420.
[65] R.D. Brown, P.D. Godfrey, D. McNaughton, A.P. Pierlot, J. Am. Chem. Soc. 110 (1988) 2329.
[66] A.L. McClellan, Tables of Experimental Dipole Moments, Rahara Enterprises, El Cerrito, CA, USA, 1989.
[67] D.A. Estrin, L. Paglieri, G. Corongiu, J. Phys. Chem. 98 (1994) 5653.
[68] J.W. Boughton, P. Pulay, Int. J. Quantum Chem. 47 (1993) 49.

[69] I.R. Gould, N.A. Burton, R.J. Hall, I.H. Hillier, J. Mol. Struct. (THEOCHEM) 331 (1995) 147.
[70] O.C. Desfranc, H. Abdoul-Carime, J.P. Schermann, J. Chem. Phys. 104 (1996) 7792.
[71] J.H. Hendricks, S.A. Lyapustina, H.L. Clercq, K.H. Bowen, J. Chem. Phys. 108 (1998) 8.
[72] M. Chahinian, H.B. Seba, B. Ancian, Chem. Phys. Lett. 285 (1998) 337.
[73] X. Hu, H. Li, W. Liang, S. Han, J. Phys. Chem. B 108 (2004) 12999.
[74] J.P. Henderson, J. Byun, J. Takeshita, J.W. Heinecke, J. Biol. Chem. 278 (2003) 23522.
[75] (a) E.S. Kryachko, M.T. Nguyen, T. Zeegers-Huyskens, J. Phys. Chem. A 105 (2001) 1934;
(b) E.S. Kryachko, M.T. Nguyen, T. Zeegers-Huyskens, J. Phys. Chem. A 105 (2001) 1288.
[76] (a) M.L. Leininger, I.M.B. Nielsen, M.E. Colvin, C.L. Janssen, J. Phys. Chem. A 106 (2002) 3850;
(b) O. Dolgounitcheva, V.G. Zakrzewski, J.V. Ortiz, Chem. Phys. Lett. 307 (1999) 220.
[77] Y. Tsuchiya, T. Tamura, M. Fujii, M. Ito, J. Phys. Chem. 92 (1988) 1760.
[78] S. Millefiori, A. Alparone, Chem. Phys. 303 (2004) 27.
[79] H. Yekeler, D. Ozbakir, J. Mol. Model. 7 (2001) 103.
[80] L. Paglieri, G. Corongiu, D.A. Estrin, Int. J. Quantum Chem. 56 (1995) 615.
[81] P. Beak, J.M. White, J. Am. Chem. Soc. 104 (1982) 7073.